Catal Lett (2012) 142:313–318
DOI 10.1007/s10562-012-0767-7

Chemical Vapor Deposition of $Pd(C_3H_5)(C_5H_5)$ to Synthesize Pd@MOF-5 Catalysts for Suzuki Coupling Reaction

Mingming Zhang · Jingchao Guan · Bingsen Zhang · Dangsheng Su · Christopher T. Williams · Changhai Liang

Received: 18 November 2011 / Accepted: 7 January 2012 / Published online: 19 January 2012

Abstract The highly porous metal organic framework MOF-5 was loaded with the metal–organic compound $[Pd(C_3H_5)(C_5H_5)]$ by metal–organic chemical vapor deposition (MOCVD) method. The inclusion compound $[Pd(C_3H_5)(C_5H_5)]$@MOF-5 was characterized by powder X-ray diffraction (PXRD), Fourier-transform infrared (FT-IR) spectroscopy, and solid-state nuclear magnetic resonance spectroscopy. It was found that the host lattice of MOF-5 remained intact upon precursor insertion. The $-C_3H_5$ ligand in the precursor is easier to lose due to the interaction between palladium and the benzenedicarboxylate linker in MOF-5, providing a possible explanation for the irreversibility of the precursor adsorption. Pd nanoparticles of about 2–5 nm in size was formed inside the cavities of MOF-5 by hydrogenolysis of the inclusion compound $[Pd(C_3H_5)(C_5H_5)]$@MOF-5 at room temperature. N_2 sorption of the obtained material confirmed that high surface area was retained. In the Suzuki coupling reaction the Pd@MOF-5 materials showed a good activity in the first catalytic run. However, the crystal structure of MOF-5 was completely destroyed during the following reaction runs, as confirmed by PXRD, which caused a big loss of the activity.

M. Zhang · J. Guan · C. Liang (✉)
Laboratory of Advanced Materials and Catalytic Engineering, Dalian University of Technology, Dalian 116024, China
e-mail: changhai@dlut.edu.cn
URL: http://finechem.dlut.edu.cn/liangchanghai

B. Zhang · D. Su
Department of Inorganic Chemistry, Fritz Haber Institute of the Max Planck Society, 14195 Berlin, Germany

C. T. Williams
Department of Chemical Engineering, University of South Carolina, Columbia, SC 29208, USA

Keywords MOF-5 · Palladium · MOCVD · Suzuki coupling

1 Introduction

Recently, there has been a considerable upsurge in the study of porous hybrid organic–inorganic materials-metal organic frameworks, referred to as MOFs. Because of their tunable cavities, high surface area, controlled porosity and low density, MOFs have been applied in a lot of fields including chemical sensing [1, 2], drug release [3], gas sorption or storage [4], and catalysis [5]. However, their application in catalysis has been very limited mainly due to two factors: first, the stability of the materials toward temperature, moisture, and some reactants and impurities is much lower compared to inorganic porous materials; second, in many MOF structures, the coordination positions around the metal ion are occupied by organic linkers, leaving no available place for reactants sorption [6–8].

However, as an alternative concept, MOF can be used as a catalyst support and applied in fine chemical synthesis. Opelt et al. [9] prepared a 0.5 wt% Pd@MOF-5 catalyst by the coprecipitation method. In the hydrogenation of ethyl cinnamate with molecular hydrogen, the activity of the sample was twice as high as that of a commercial Pd/C catalyst with the same Pd content. Sabo et al. [10] deposited 1 wt% Pd on MOF-5 by an incipient wetness method and the sample exhibited higher activity in the hydrogenation of styrene compared to conventional 1 wt% Pd/C catalysts. Schröder et al. [11] reported a Ru@MOF-5 catalyst prepared by metal–organic chemical vapor deposition (MOCVD) method, in which the Ru particles had about a narrow size range of 1.5–1.7 nm. The sample was used as a catalyst for alcohol oxidation, and the kinetic data revealed

the limitation of the water-sensitive MOF-5 host material for catalytic applications. Hermes et al. [12] also generated Pd nanocrystallites of about 1.4 nm size on MOF-5 via the MOCVD method. The sample contained a very high loading of 36 wt%, but was only weakly active in the hydrogenation of cyclooctene.

As a catalyst support, MOF-5 has been used in hydrogenation [8], polymerization [13], and isomerization reactions [14]. However, its use in C–C bond coupling reactions is very limited. Gao et al. [15] used a heterogeneous Pd@MOF-5 catalyst by immersion method in ligand- and copper- free Sonogashira coupling reactions. The sample showed a high activity and stability through several uses. Few reports have been found for application of MOF-5 in Suzuki reaction, which is perhaps the most powerful and versatile method for formation of new biaryls [16–18].

In this work, MOF-5 is employed as a support for Pd supported catalysts prepared by MOCVD method. MOF-5 is a typical and common representative among the array of MOF materials available, consisting of Zn_4O^{6+} clusters as metal nodes and benzene-1,4-dicarboxylate as organic linker [19]. A highly volatile palladium metal–organic complex [$Pd(C_3H_5)(C_5H_5)$] was chosen as the precursor. The resulting supported Pd catalyst showed good initial activity for Suzuki reaction in the solvent of DMF with K_2CO_3 as base, before suffering from deactivation due to the instability of the pore structure in the MOF-5 support.

2 Experimental

2.1 Synthesis

Samples of MOF-5 [20] and [$Pd(C_3H_5)(C_5H_5)$] [21, 22] were synthesized according to literature reports. The loading of MOF-5 with the volatile [$Pd(C_3H_5)(C_5H_5)$] followed the procedure described by Hermes [11] with some modifications. 500 mg of freshly activated MOF-5 and a certain amount of the precursor were mixed together in a Schlenk bottle, which was then evacuated to 1 Pa. The loading was carried out under static vacuum at room temperature for 10 h. The hydrogenation procedure was operated in a long glass tube with a sieve plate. The sample of [$Pd(C_3H_5)(C_5H_5)$]@MOF-5 was placed on the sieve plate with H_2 passing through for 1 h, at which point the gas was switched to Ar and kept for 1 h.

2.2 Catalytic Reaction

The general procedure for the Pd@MOF-5-catalyzed Suzuki coupling reaction was as follows. A 100 mL three necked flask was charged with Pd@MOF-5 (50 mg) and a certain base and purged with Ar. The solvent (10 mL) and phenylboronic acid (1.1 mmol) were added followed by bromobenzene (1.0 mmol). The flask was maintained at 90 °C in an oil bath and stirred for appropriate time. The reaction products were analyzed by GC.

2.3 Characterization

Powder X-ray diffraction (PXRD) was carried out using a D/MAX 2400 diffractometer with Cu Kα monochromatized radiation source ($\lambda = 1.5418$ Å) operated at 40 kV and 100 mA. Fourier transform infrared (FT-IR) spectra were collected at room temperature on a Nicolet Impact 410 with a resolution of 4 cm^{-1}. The surface area, pore volume, and pore size distribution of the support and catalyst were determined from nitrogen adsorption–desorption isotherms at −196 °C using a Micromeritics 2020 apparatus. A FEI Cs-corrected Titan 80-300 microscope was employed to acquire TEM images operated at 80 kV. Finally, ^{13}C MAS NMR spectra were recorded on Bruker DSX 400 MHz instrument in ZrO_2 rotors with a rotational frequency of 8 kHz.

3 Results and Discussion

3.1 Loading of MOF-5 with [$Pd(C_3H_5)(C_5H_5)$]

The [$Pd(C_3H_5)(C_5H_5)$] precursor was selected because of its high volatility and low decomposition temperature under H_2. This compound can be sublimed without decomposition at room temperature under 6×10^{-2} Pa. Thus, the loading process was carried out under static vacuum (6×10^{-2} Pa) at room temperature (23 °C) for 10 h. Different from other reports [11, 12, 23] in which the metallic precursor was in high excess, [$Pd(C_3H_5)(C_5H_5)$] was added in a certain mass ratio (1, 2.5, 5 and 10%).

The XRD pattern of [$Pd(C_3H_5)(C_5H_5)$]@MOF-5 (Fig. 1) shows almost no difference from the pattern of pure activated MOF-5, which indicates that MOF-5 is intact after the loading process. The intensity ratio of reflections at $2\theta = 6.9°$ and 9.7° is lowered upon inclusion of the precursor, which is a commonly observed phenomenon on MOF-5 when the pore canal is occupied by guest molecules [24].

The FT-IR spectra of pure MOF-5 and the intercalation compound [$Pd(C_3H_5)(C_5H_5)$]@MOF-5 are shown in Fig. 2. The strong bands at 1511, 1581 and 1607 cm^{-1} are ascribed to the asymmetric stretching of carboxyl group of the BDC linker in MOF-5. The band at 1,397 cm^{-1} is attributed to symmetric stretching of the carboxyl group. The signals of the out of plane vibrations of the BDC linker are observed at 1018, 889, 823 and 748 cm^{-1}. The

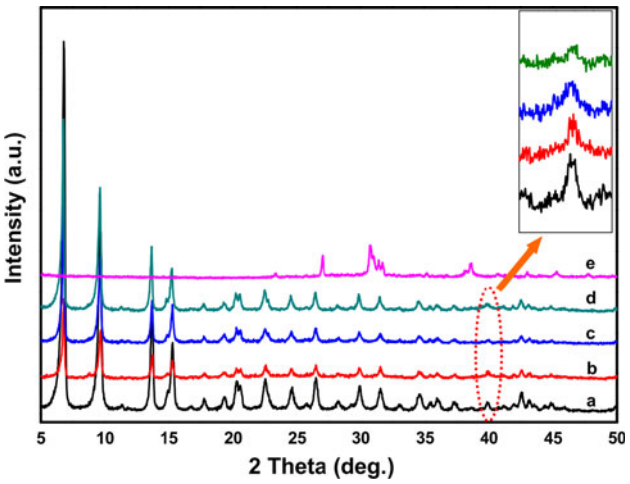

Fig. 1 XRD patterns of MOF-5 (*a*), $Pd(C_3H_5)(C_5H_5)$@MOF-5 (*b*), and Pd@MOF-5 before (*c* 0.69 wt% Pd, *d* 1.3 wt% Pd) and after reaction (*e*)

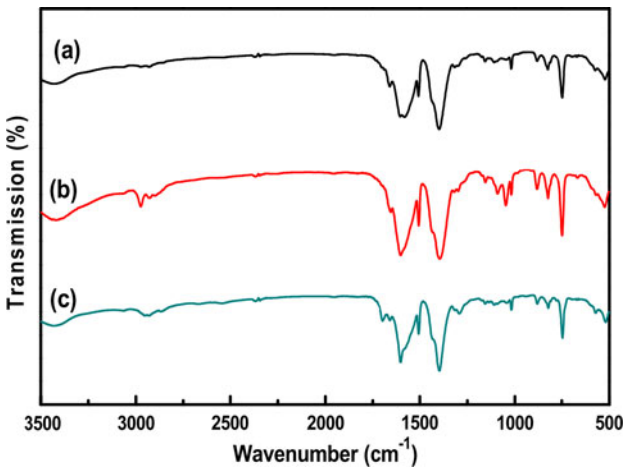

Fig. 2 FT-IR of pure MOF-5 (*a*), $Pd(C_3H_5)$ (C_5H_5) @MOF-5 (*b*), Pd@MOF-5 (*c*)

intercalation compound still exhibits all the bands of pure MOF-5, which indicates that the support material has remained intact. Several new bands at 1050, 1093 and 1161 cm^{-1} appeared due to the out of plane vibrations of the cyclopentadiene group in the precursor. The new emerged at 2,980 cm^{-1} can be caused by symmetric stretching of the allylic C–H bond in the precursor.

The ^{13}C MAS NMR spectra of pure MOF-5, $[Pd(C_3H_5)(C_5H_5)]$ and inclusion compound $[Pd(C_3H_5)(C_5H_5)]$@MOF-5 are given in Fig. 3. The carbon resonance signals of the bdc (1,4-benzenedicarboxylate) linker in MOF-5 are found at 175.3 (COO), 136.7 (C(COO)), and 131.2 (C_6H_6) ppm, which are consistent with published information for pure MOF-5 [12]. The characteristic signals of $[Pd(C_3H_5)(C_5H_5)]$ are shown at 96.6 (C_5H_5) and 49.1 (C_3H_5) ppm. After inclusion, it is found that the signal of C_3H_5 is missing.

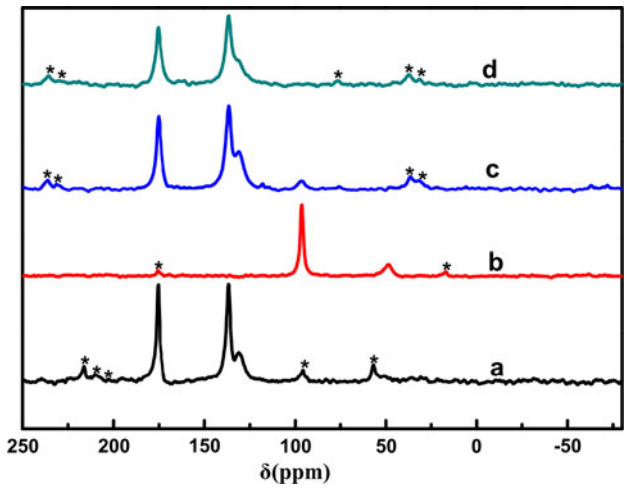

Fig. 3 ^{13}C MAS NMR spectra of MOF-5 (*a*), $Pd(C_3H_5)(C_5H_5)$ (*b*), $Pd(C_3H_5)(C_5H_5)$@MOF-5 (*c*), and Pd@MOF-5 (*d*). The signals with "*asterisk*" are spinning sidebands

It is known that the $[Pd(C_3H_5)(C_5H_5)]$@MOF-5 can be turned to Pd@MOF-5 by photolysis [11]. A color change from pink to brown of the compound was also observed in our experiment. So it is obvious that the $[Pd(C_3H_5)(C_5H_5)]$ started to decompose at room temperature when exposed to light. According to the ^{13}C MAS NMR spectrum it can be deduced that the functional group of $–C_3H_5$ is more unstable than $–C_5H_5$ during this decomposition. This may be the reason why the palladium compound adsorption process is not reversible, as opposed to the $FeCp_2$ precursor [13]. This facile liberation of the $–C_3H_5$ allows the palladium to more readily coordinate with the bdc link in MOF-5, thus trapping the precursor in the cage. A similar phenomenon was also found by Esken et al. [12] for a Ru(cod)(cot) (cod = 1,5-cyclooctadiene, cot = 1,3,5-cyclooctatriene) precursor. They found that the precursor preferred to lose the cot ligand first, thus leaving the [Ru(cod)] fragment that could be coordinated to bdc linker in MOF-5. They referred to this phenomenon as a "caging" effect of MOF-5. However, in their work they did not describe this effect for Pd@MOF-5.

3.2 Reduction of $[Pd(C_3H_5)(C_5H_5)]$@MOF-5

Four samples with different Pd loading amounts (0.17, 0.69, 1.3, and 4.2 wt%) as determined by Inductively Coupled Plasma-Atomic Emission Spectrometry (ICP-AES) analysis were prepared. The XRD patterns of Pd@MOF-5 (0.7 wt% Pd and 1.3 wt% Pd) are shown in Fig. 1. The characteristic signals of MOF-5 show no apparent difference after the hydrolysis process, except that the intensity of all peaks is strengthened. The characteristic peaks of palladium are not obviously found due to the low loading amounts and the good distribution [25]. However,

the broadened signal at $2\theta = 40.0°$ is assigned to an effect caused by the insertion of palladium [26].

The FT-IR spectrum of Pd@MOF-5 compared to $[Pd(C_3H_5)(C_5H_5)]$@MOF-5 and pure MOF-5 is shown in Fig. 2. The bands from the palladium precursor disappeared completely after the reduction process. However, the signals of MOF-5 remained, except for some new bands at 1,698 and 1,290 cm^{-1}. These can be explained by the trace amounts of hydrocarbon by-products remaining in MOF-5 after the precursor decomposition.

In the ^{13}C MAS NMR spectrum (Fig. 3), the sample of Pd@MOF-5 only reveals the characteristic resonances of intact MOF-5 at 175.3 (COO), 136.7 (C(COO)), and 131.2 (C_6H_6) ppm. No hydrocarbon impurities or hydrogenation of bdc linkers can be detected in ^{13}C NMR spectrum.

The $Pd_{3d3/2}$ and $Pd_{3d5/2}$ XPS spectrum of Pd@MOF-5 is shown in Fig. 4. It is observed that the $Pd_{3d3/2}$ and $Pd_{3d5/2}$ regions can both be deconvoluted into two peaks, which indicates the existence of two different palladium species. According to the NIST XPS Database, the Pd with the binding energy at 340.4 eV (3d3/2) is characteristic of PdOx/Pd [27] and 335.8 eV (3d5/2) is characteristic of PdO [28]. The signals at 341.1 eV (3d3/2) and 334.9 eV (3d5/2) are characteristic of Pd metal [29, 30]. The results reveal that the Pd in MOF-5 is so activated that a considerable amount of the metal is oxidized to PdO.

The N_2 sorption isotherms and pore size distributions were measured for MOF-5 with and without Pd at 77 K (Fig. 5). The data of the inclusion compound $[Pd(C_3H_5)(C_5H_5)]$@MOF-5 are not given because the precursor would be decomposed at the desorption temperature (200 °C) [22]. Type I isotherms according to IUPAC classification were observed, which are typical for microporous materials. MOF-5 exhibited a Brunauer–Emmett–Teller (BET) surface area of 316 m^2/g, which slightly decreased after Pd loading.

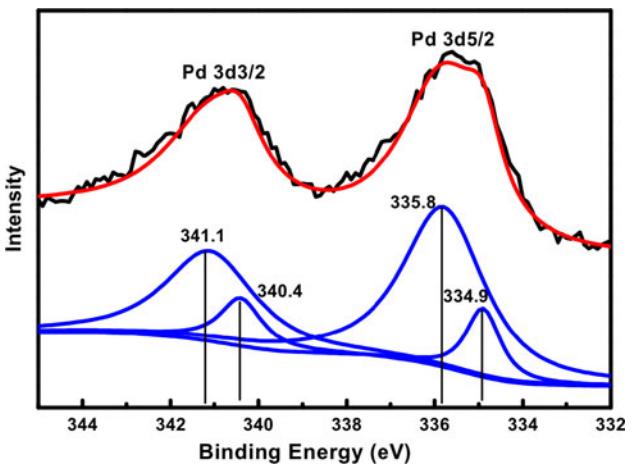

Fig. 4 XPS of Pd@MOF-5. *Black* is the original pattern. *Red* is the simulated pattern. *Blue lines* are deconvoluted peaks

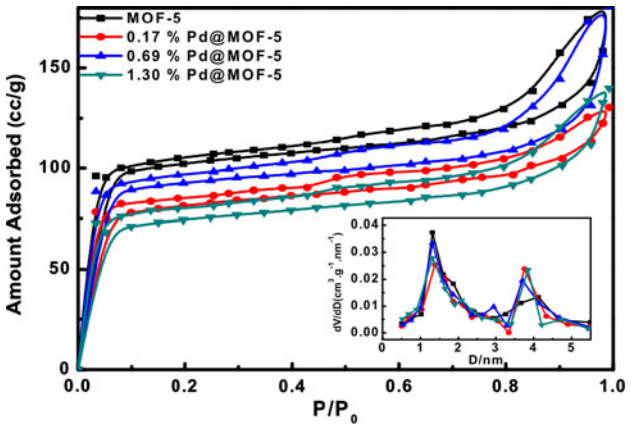

Fig. 5 N_2 adsorption desorption isotherms and pore size distributions of MOF-5 and Pd@MOF-5

The pore size distributions prove that there are two types of micropores in the range of 1–2 and 3.5–4.2 nm. Loading of Pd reduces the number of micropores with smaller size, while simultaneously creates larger micropores, which indirectly prove that the Pd particles are not just formed on the surface of MOF-5. The TEM images also show that the Pd particles are mostly grown in the canal of MOF-5. It has been proven that the characteristic reflections for MOF-5 framework in the XRD would be reduced or completely missing while the high surface area is still left when the Pd loading is up to 26.4% (ref. 12). So the long-range order of the MOF-5 host can be destroyed by the loading of Pd. But in this paper, the Pd loading is much lower. The damage to MOF-5 is so little that's why only small differences can be detected in N_2 adsorption results but no apparent differences can be seen from XRD, FT-IR and NMR data.

The TEM images of MOF-5 and Pd@MOF-5 are shown in Fig. 6. The typical rectangular shapes of MOF-5 crystallites can still be revealed in both MOF-5 and Pd@MOF-5 TEM images, indicating that the MOF-5 crystal structure is intact under the relatively low electron beam dosage (80 kV). The typical size of the embedded Pd particles is around 2–5 nm. The particles are well dispersed in the canal of MOF-5 and no apparent aggregation on the surface of MOF-5 can be seen. It has been proven that when the Pd loading is high, the Pd particles can fully spread though the MOF-5 matrix [31]. In this work the Pd loading is much lower, because of which some of the particles are formed near the surface of MOF-5.

3.3 Suzuki Coupling Reaction over Pd@MOF-5

Phenylboronic acid and bromobenzene were chosen as the substrates to investigate the catalytic performance of Pd@MOF-5. Initially, DMF was chosen as the solvent to research the appropriate base. The organic base triethylamine was

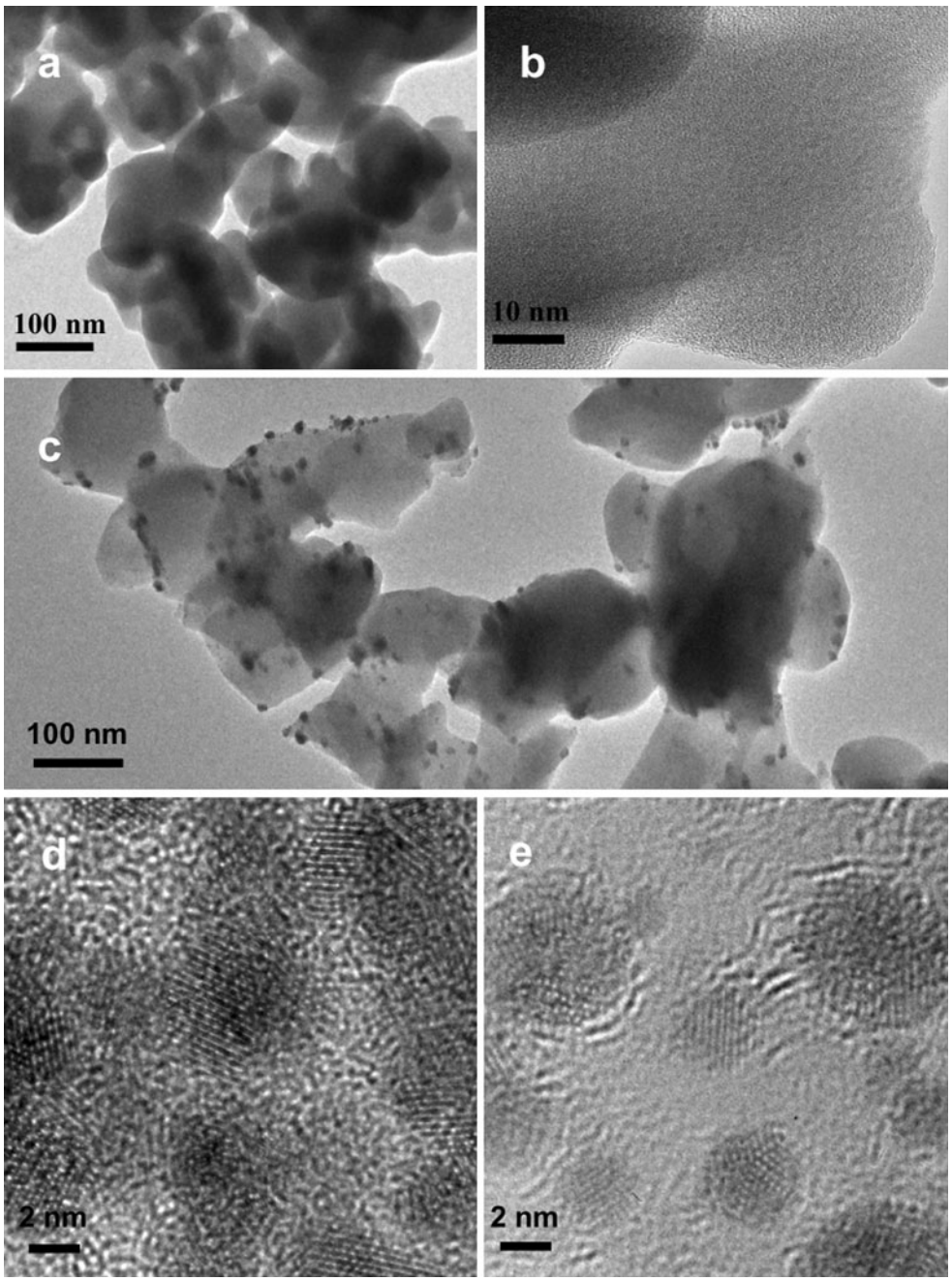

Fig. 6 TEM images of MOF-5 (**a**, **b**) and Pd@MOF-5 before (**c**, **d**) and after reaction (**e**)

firstly chosen, since an organic solvent was used, but almost no transformation was observed. Then some typical inorganic bases—$NaHCO_3$, Na_2CO_3, Na_3PO_4 and K_2CO_3—were selected. It was found that very low yield was obtained by $NaHCO_3$ and Na_2CO_3 due to their relatively low basicity and only Na_3PO_4 and K_2CO_3 gave a good activity. Different solvents were also investigated. Since the support of MOF-5 is very sensitive to water, the reaction can only be carried out in organic solvents. Several organic solvents were tested, with acetone and ethanol achieving only very low conversion, and CH_3OH achieving almost the same yield as DMF. The effects of different solvents and bases are shown in Table 1.

The effect of Pd loading on the catalytic performance was tested in DMF solvent with K_2CO_3 as the base. The condition for the reaction was at 90 °C for 20 h. When the loading amount was 0.17 wt%, the conversion was very low. The conversion considerably increased when the loading amount was higher, rising to 81% yield at 4.2 wt%. A significant decrease of the activity is observed in second run, with further runs resulting in much smaller negative effect. The results are summarized in Table 2. The

Table 1 Effects of solvents and bases on Suzuki reaction

Solvent	Base	*t* (h)	*T* (°C)	Conversion (%)
DMF	Triethylamine	20	90	<1
DMF	$NaHCO_3$	20	90	<1
DMF	Na_2CO_3	20	90	<1
DMF	K_2CO_3	20	90	81
DMF	Na_3PO_4	20	90	72
CH_3OH	K_2CO_3	20	90	76
Acetone	K_2CO_3	20	90	<1
Ethanol	K_2CO_3	20	90	20

Table 2 Effect of Pd loading on catalytic performance and reusability

Entry	Run	*t* (h)	Conversion (%)			
			0.17% Pd	0.69% Pd	1.3% Pd	4.2% Pd
1	1	20	7	23	48	81
2	2	20	n.t.	n.t.	n.t.	38
3	3	20	n.t.	n.t.	n.t.	29
4	4	20	n.t.	n.t.	n.t.	21

n.t. = not tested

characteristic reflections for MOF-5 in the XRD of the sample after the first run were completely missing as shown in Fig. 1e. However, no particle growing or aggregation is found after reaction from the TEM results (Fig. 5e). Thus, it is speculated that the collapse of the pore canals in MOF-5 is the main reason for the drop of the activity.

4 Conclusion

The embedding of palladium nanoparticles into the metal organic framework MOF-5 has been successfully prepared by metal–organic chemical vapor deposition method, and been used as catalyst for Suzuki reaction. The XRD and ^{13}C MAS NMR results all revealed that the MOF-5 was intact after MOCVD and reduction procedure. The prepared Pd@MOF-5 had a very high BET surface area with Pd particles in size of 2–5 nm. The precursor was easier to lose $–C_3H_5$ ligand than to lose $–C_5H_5$, which may explain why the precursor adsorption process is not reversible. The Pd@MOF-5 was used as a heterogeneous catalyst for the Suzuki coupling reaction and achieved a good activity in the first run. The activity significantly decreased in the second run and dropped slowly in the following runs, which was confirmed that the collapse of pore canals in MOF-5 was the main reason for the weak performance of the reused catalysts.

Acknowledgments We gratefully acknowledge the financial support provided by the National Natural Science Foundation of China (No. 21073023). C.T.W. thanks Dalian University of Technology for a "Seasky" professorship.

References

1. Bauer CA, Timofeeva TV, Settersten TB, Patterson BD, Liu VH, Simmons BA, Allendorf MD (2007) J Am Chem Soc 129:7136
2. Chen B, Yang Y, Zapata F, Lin G, Qian G, Lobkovsky EB (2007) Adv Mater 19:1693
3. Horcajada P, Serre C, Vallet-Regí M, Sebban M, Taulelle F, Férey G (2006) Angew Chem Int Ed 45:5974
4. Mueller U, Schubert M, Teich F, Puetter H, Schierle-Arndt K, Pastré J (2006) J Mater Chem 16:626
5. Cho SH, Ma B, Nguyen ST, Hupp JT, Albrecht-Schmitt TE (2006) Chem Commun 24:2563
6. Llabrés i Xamena FX, Abad A, Corma A, Garcia H (2007) J Catal 250:294
7. Llabrés i Xamena FX, Xamena FX, Corma A, Garcia H (2007) J Phys Chem C 111:80
8. Alaerts L, Seguin E, Poelman H, Thibault-Starzyk F, Jacobs PA, De Vos DE (2006) Chem Eur J 12:7353
9. Opelt S, Türk S, Dietzsch E, Henschel A, Kaskel S, Klemm E (2008) Catal Commun 9:1286
10. Sabo M, Henschel A, Fröede H, Klemm E, Kaskel S (2007) J Mater Chem 17:3827
11. Schröder F, Esken D, Cokoja M, van den Berg MWE, Lebedev OI, Tendeloo GV, Walaszek B, Buntkowsky G, Limbach H, Chaudret B, Fischer RA (2008) J Am Chem Soc 130:6119
12. Hermes S, Schröder MK, Schmid R, Khodeir L, Muhler M, Tissler A, Fischer RW, Fischer RA (2005) Angew Chem Int Ed 44:6237
13. Perles LJ, Iglesias M, Martin-Luengo MA, Monge MA, Ruiz-Valero C, Snejko N (2005) Chem Mater 17:5837
14. Schlichte K, Kratzke T, Kaskel S (2004) Microporous Mesoporous Mater 73:81
15. Gao SX, Zhao N, Shu MH, Che SA (2010) Appl Catal A 388:196
16. Miyaura N, Suzuki A (1995) Chem Rev 95:2457
17. Stanforth SP (1998) Tetrahedron 54:263
18. Han J, Liu Y, Guo R (2009) J Am Chem Soc 131:2060
19. Li HL, Eddaoudi M, O'Keeffe M, Yaghi OM (1999) Nature 402:276
20. Tranchemontagne DJ, Hunt JR, Yaghi OM (2008) Tetrahedron 64:8553
21. Dent WT, Long R, Wilkinson AJ (1964) J Chem Soc 8:1585
22. Shaw BL (1960) Proc Chem Soc 7:247
23. Müller M, Lebedev OI, Fischer RA (2008) J Mater Chem 18:5274
24. Jasmina H, Morten B, Unni O (2007) J Am Chem Soc 129:3612
25. Wan Y, Wang H, Zhao Q, Klingstedt O, Terasaki O, Zhao D (2009) J Am Chem Soc 131:4541
26. Esken D, Zhang XN, Lebedev OI, Schröder F, Fischer RA (2009) J Mater Chem 19:1314–1319
27. Moddeman WE, Bowling WC, Carter DC, Grove DR (1988) Surf Interface Anal 11:317
28. Sakurada O, Takahashi H, Taga M (1980) Bunseki Kagaku 38:407
29. Tressaud A, Khairoun S, Touhara H, Watanabe NZ (1986) Anorg Allg Chem 291:540
30. Budhani RC, Banerjee A, Goel TC, Chopra KL (1983) J Noncryst Solids 55:93
31. Turner S, Lebedev OI, Schröder F, Esken D, Fischer RA, Tendeloo GV (2008) Chem Mater 20:5622